Eur. Phys. J. D **43**, 91–95 (2007)
DOI: 10.1140/epjd/e2007-00117-6

THE EUROPEAN PHYSICAL JOURNAL D

The colours of nanometric gold

Optical response functions of selected gold-cluster thiolates

R.B. Wyrwas[a], M.M. Alvarez[b], J.T. Khoury[b], R.C. Price, T.G. Schaaff[c], and R.L. Whetten[d]

School of Chemistry & Biochemistry, Georgia Institute of Technology, Atlanta, GA 30332-0400, USA

Received 25 August 2006 / Received in final form 2nd October 2006
Published online 24 May 2007

Abstract. A set of broad-range NIR-vis-UV optical absorption spectra, measured for selected gold-cluster thiolate compounds (*GCTs*, containing ∼20 to 300 Au atoms), is consistently displayed and then analyzed within the dielectric-functions approach. The size-evolution toward 'bulk' (Au diameter > 3-nm) optical response is thereby clearly demonstrated. The emergence of apparent energy gaps, E_{on}, for onset of optical absorption, as well as other fine-structure, is consistent with that of a well-quantized *metallic* electronic structure for the compounds' cores: the onset-band's location E_{on} and intensity are attributed semiclassically to a circulation-frequency resonance of the Fermi-level electrons. With decreasing cluster-size, an increasing fraction of the integrated (sum-rule) intensity is 'missing' from the < 4 eV region. This might be explained by the outermost layer consisting of Au(I)thiolate complexes.

PACS. 73.22.-f Electronic structure of nanoscale materials: clusters, nanoparticles, nanotubes, and nanocrystals – 73.22.Lp Collective excitations – 36.40.Vz Optical properties of clusters – 78.20.Ci Optical constants (including refractive index, complex dielectric constant, absorption, reflection and transmission coefficients, emissivity)

1 Introduction

Many reasons are given for the great current interest in the optical properties of nm-scale gold particles, generally, and for those of the gold-cluster thiolate (GCT) series, in particular [1]. For the present purpose, it suffices to recall that their optical-spectroscopic properties serve as a key means to distinguish them, as well as to discuss the size-evolution of their electronic properties, yet these properties were often misinterpreted (*vide infra*). The main contribution of this report is to display a consistent set of illustrations of selected spectra and the associated response functions, such that well-founded conclusions can be drawn [2]. Whereas the size and composition of compounds in this series (see Table) are increasingly well established [3], a general understanding of their structure and bonding remains limited. Thus the correct spectral analysis also may be valuable for clarifying these issues.

[a] *Permanent address*: Departement of Chemistry, Indiana University, Bloomington, IN 47405-7102, USA.
[b] *Permanent address*: Research Division, Los Angeles County Sanitation District, Los Angeles, CA 90607, USA.
[c] *Permanent address*: Chemical Sciences Division-Oak Ridge National Laboratory, Oak Ridge, TN 37831, USA.
[d] e-mail: `whetten@chemistry.gatech.edu`

2 Absorption coefficients, vs. wavelength and frequency

Optical absorption spectra, $A(\lambda)$, are obtained using NIR-vis-UV spectrometers that scan linearly with optical wavelength (λ, in nm), usually for dilute solution-phase samples. Because the spectra cover a very wide range, 300–1400 nm or wider, it is convenient to display them instead vs. frequency (ω, cm^{-1}), or equivalently, photon energy (E, eV), covering the range 0.8–4.0 eV. This has the unfortunate consequence that the (integrated) intensities of features in diverse spectral regions can no longer be compared (nor can *sum-rules* be obeyed, *vide infra*), *unless* the intensities are scaled by the appropriate factor, namely λ^2, or equivalently E^{-2}, e.g. $I(E) = E^{-2}A(\lambda(\mathrm{E}))$. Figure 1a displays such suitably corrected spectra, for the selected set of GCT compounds [4]. Comparison with published articles, in which this correction-factor is not applied, confirms that its effect is very substantial, e.g. a ∼20-fold exaggeration of UV-band intensity over NIR-bands. The same considerations apply to the common practice of displaying differential spectral intensity vs. frequency (or energy), whether they are obtained numerically ($dA/d\lambda$) or instrumentally, as in circular dichroism (CD) spectra [5].

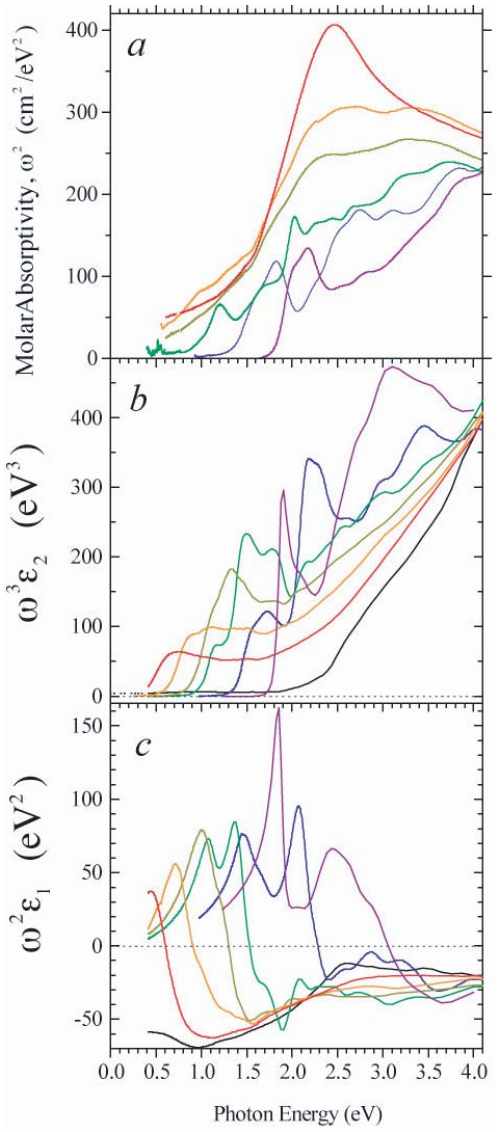

Fig. 1. (Color online) Optical signatures. (a) Absorptivity (per mole of Au atoms). Imaginary (b) and real (c) parts of the complex dielectric functions extracted from the dispersion analysis of the experimental absorption spectra. The ω^{-2}, ω^3, and ω^2 scaling deconvolutes Drude-type behavior. O+: purple; I: blue; II: green; III: yellow: V: orange; VIII: red; bulk (Johnson and Christy): black.

3 Comparison to 'bulk' properties: extraction of optical dielectric functions

The observed spectral properties of 'bulk' *fcc*-gold are defined as those arising from its optical dielectric function, $\varepsilon(\omega)$, along with that of the surrounding medium (vacuum, dielectric) [6]. So the 'size-evolution to bulk' is best analyzed using this function. Its component functions (real-ε_1, imaginary-ε_2) are displayed in Figure 1, along with those derived (as explained in the caption), for the selected *GCTs*. Because the bulk functions diverge at low frequency (IR), it is helpful to rescale them as indicated. With this, the clear similarities (UV) as well as striking differences (NIR), become immediately evident; among the latter are: emergence of discrete spectral structure (bands); enormous enhancement of NIR response; and emergence of an apparent onset (minimum energy, E_{on}) of optical absorption. By contrast, it is well established that, in this sense, the optical response of room-temperature colloidal-gold is 'bulk' down to at least 3-nm, when a simple modification is introduced within the ubiquitous 'mean-free-path hypothesis' [7].

Although the results of this procedure cannot be taken too literally — a cluster of only ∼1.0-nm diameter can hardly be regarded as a sphere with a uniform dielectric-function within and a uniform dielectric without — they can be consistently deduced, and have evident utility, as described extensively by Kreibig et al. [8], who stress that it answers the question: what would the dielectric functions of a uniform cluster need to be, in order that it reproduce the complete optical-absorption spectrum, along with other reasonable criteria? Plus these procedures are conveniently incorporated with those needed to estimate static polarizability, integrated (sum-rule) intensity, and so on.

4 Extracted quantities: sum-rule intensities, E_{on} and other fine-structure

Given a consistently rendered set of spectral functions, one can extract certain key quantities and display them as a function of size. Perhaps the most important of these are the integrated absorption coefficient (sum-rule intensity, *SRI*) and the energy E_{on} of the apparent onset of measurable absorption intensity. These quantities are plotted, in the usual manner, in the panels of Figure 2. The absorption intensity, expressed on a per-Au-atom basis and integrated across the 0.4–4 eV range, i.e. where the conduction-electron response is expected to be mainly exhausted, falls strongly with decreasing cluster size (Fig. 2a). This perplexing result is discussed in the concluding section below.

For the E_{on} plot, one uses either the imaginary (onset) or real (zero) function; other features, above the absorption onset, can be similarly deduced. Yet another method is available, at least for the smaller sizes, and that is to use the max/min energies from the *CD* spectra. These provide the clearest evidence to date that the spectral features should be regarded as arising from a sequence of discrete electronic transitions each of definite character, rather than as a 'structured continuum'. It remains an open challenge to assign these transitions.

5 Comparison to theory

5.1 Jellium-model results, and circulation-frequency model

First, one must note the widespread uncertainty over the extent to which the optical spectra can be used to draw

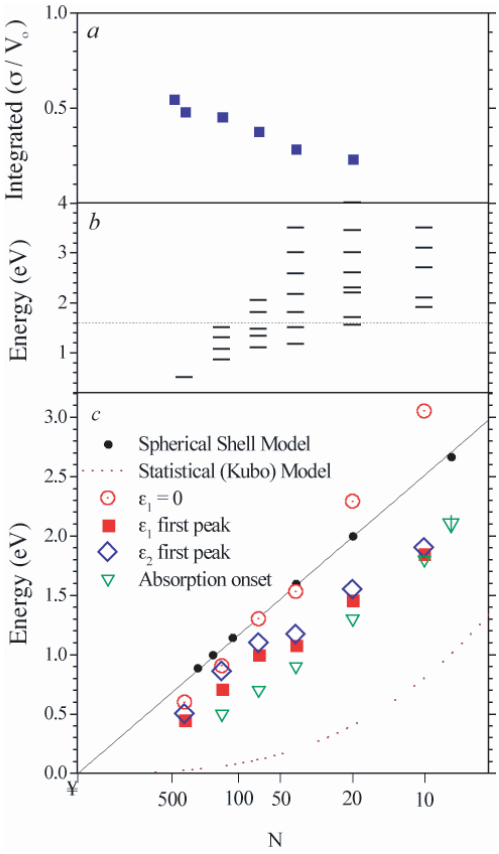

Fig. 2. (Color online) Significant spectral features. (a) Integrated absorption cross-section (0.4 to 4 eV) normalized to the sum-rule value for spherical metal particles of equivalent diameter. (b) Salient peak positions (structure) in ε_2; the dotted line marks the interband transition onset (1.7 eV) for bulk gold. (c) Experimental onset of absorption is compared to theoretical predictions (spherical shell, Kubo); also shown are the demarcation point for anomalous dispersion ($\varepsilon_1 = 0$), and the first peak in ε_1 and ε_2. Legend: (-•-) band gap from spherical shell model; (....) Kubo gap; (∇) onset of absorption from the imaginary part of the dielectric function; ($\circ$) anomalous dispersion; (■) first peak in ε_1; ($\diamond$) first spectral band in ε_2.

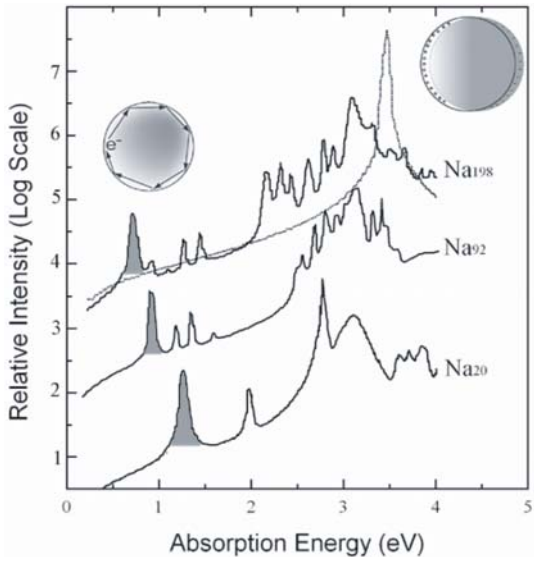

Fig. 3. TD-DFT calculations of Na_{20}, Na_{92}, and Na_{198}. See references [10,11] for computational details. The lowest energy transition is independent of the *GDR/SPR* peak and is dependent on the size of the particle. In a semi-classical approach, the path of the conduction electrons can be considered to travel the circumference of the particle near the Fermi energy. Any transition from the ground state, (n, l_o) to $(n, l_o{+}1)$, would satisfy the electric-dipole selection rule $\Delta l = +1$, therefore being an allowed transition. The energy of such states are dominated primarily by centripetal motion and the transition energy can be defined as $\Delta E_{l_o \to l_o+1} \approx \frac{\hbar^2}{2m_e R^2}\,(2l_o + 1)$, where R is the particle radius. In term of a bulk parameter, the Fermi velocity, v_F, an angular momentum can be defined as $\hbar l_F = m v_F R$, where $l_F \cong l_o + \frac{1}{2}$. The term l_F could be used to quantify the angular momentum at the Fermi velocity and is neither l_o or $(l_o + 1)$ instead some point in between. The final substitution of l_F gives the final transition energy to be $E_{on} \approx h v_f / \pi D$.

conclusions about the electronic structure and bonding in *GCT*-compounds: invocations of 'quantum size-effect' (*QSE*) vie with terms such as 'non-metallic' or 'metal-to-insulator transition', where the latter conclusions are often inferred from little more than the observed presence/absence of a visible absorption maximum (giant-dipole 'plasmon' resonance, *GDR/SPR*) or an absorption onset ('gap') in the *NIR* [9]. In this context, it is useful here to compare the spectral-response functions, as consistently and systematically deduced, to what is expected from a sampling of robust and high-level theoretical results, and also to recast those results in clearly comprehensible terms.

Figure 3 illustrates the general trend from 'jellium'-model TD-DFT calculations [10,11]. Such models epitomize the *QSE*s of the metallic state: All valence (conduction) electrons interact self-consistently, with a high degree of 'correlation', in the background of a uniformly charged *sphere/spheroid* of (cat)ion charge density (beware the log(10)-scale). Note that both the *GDR/SPR* resonance, smeared out at higher energy, and a sequence of much weaker low-energy resonances are evident. These discrete resonances can be assigned to (electron-hole) transitions among the electronic shells (n, l) of the spherical 'superatom'.

Figure 4 plots E_{on}, vs. diameter, as obtained from the lowest-energy resonance in such calculations; and incorporates the present E_{on} values for the *GCT*-compounds (Fig. 3, *upper*). The important point here is that there is no great discrepancy between the fully 'metallic' model and the observed cluster responses, if one assumes that closed electronic shells and spherical symmetry are approximately valid. There is an evident distinction between this well-quantized 'metallic' electronic structure and the better-established case of well-quantized 'semiconductor' electronic structure (parabolic curve), even in the case where the latter's bandgap is quite small, e.g. PbS. And, of course, the above-onset behavior of semiconductor nanoparticles is also much simpler and well understood,

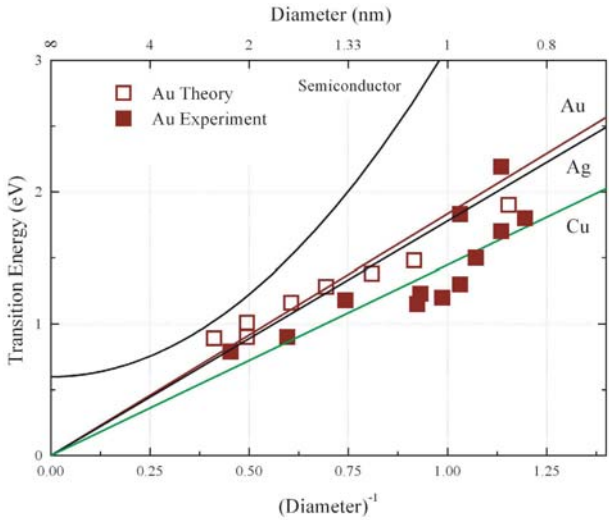

Fig. 4. E_{on} versus D^{-1}. The E_{on} values, calculated as derived in Figure 3, plotted as a function of the diameter of the nanoparticles for gold, silver and copper show the linear increase with decreasing diameter. Theoretical E_{on} values (open squares) and measured E_{on} values (filled squares) are plotted for comparison. As mentioned in Section 3, the particles can hardly be considered purely spherical, hence the deviation. For comparison, the non-linear response representing the band-gap energy dependence of semi-conductor nanoparticles as a function of size is included.

in terms of the unoccupied conduction-band's (S-P-D-F...) level-structure [12].

The straight lines (one for each metal), are given by $E_{on}/h = v_F/\pi D$, where v_F is the (Fermi) velocity of the bulk metal, and the denominator is the cluster's circumference (see Fig. 3). Thus the first absorption band may be interpreted semi-classically as circulation-frequency resonance. Such a simple (approximate) result arises when the dominant onset transition is of the $(n = 1, l_{max})$ to $(n + 1, l_{max} + 1)$, which are always allowed by electric-dipole selection rules [13].

5.2 'Missing' sum-rule intensity as electronic-structure evidence

The missing intensity could of course simply be shifted toward higher energy (beyond 4 eV), an idea given explicit credence by the work of Lermé et al. [14]. However, the magnitude of the effect suggests that the cause of such a shift would be the oxidation of a fraction of the gold atoms, as suggested also in earlier theoretical work [15]. Very recently, Häkkinen, Walter and Grönbeck [16,17] have proposed a striking new variant on this theme, in which the cluster-compound may be divided into two spatial (structure/bonding) regions: a metallic [Au(0)] core, that responds much like the electronic shell model (e.g. jellium calculations above), and a weakly coordinating nonmetallic-stoichiometric [Au(I)SR] mantle. The latter has roughly all its absorption intensity above 4 eV.

Table 1. Sample characteristics. Masses are in kDa (1000 amu) and gold core mean geometrical diameters in nm — as determined from mass spectrometry, HRTEM, and XRD analyses. Composition refers to the number of gold atoms (nAu): thiols (mSR): charges (z) ($n_e = n\mathrm{Au} - m\mathrm{SR} + z$). A raw mixture of these molecules is prepared by reductive decomposition of polymeric AuSR compounds. Individual fractions are purified by fractional crystallization, column chromatography, or gel-electrophoresis, as appropriate to their size and R-group. [a] Adsorbed group, [b] diameter from $(\pi/6)\, D_{eq}^3\, n_{\mathrm{Au}}^{fcc} = N_{\mathrm{Au}}$, [c] method of isolation, [d] glutathione, [e] gel electrophoresis, [f] gel chromatography, [g] hexanethiol, [h] column chromatography, [i] recrystalization, [j] dodecanethiol, [k] fractional recrystalization, [l] appearance in solution.

	Mass Compsn n_e	Thio-[a]	D_{eq} [b]	Colour[l]	Method[c]
0^+	4 20:14:0 6	SG[d]	0.9	Rose	EP[e]
I	6 25:18:1 8	SG	1.0	Orange	EP
II	8 39:23:2 18	SC_6^g	1.1	Honey	CC[h]
III	14 75:42:1 34	SC_6	1.38	Green	RC[i]
V	29 152:60:0 92	SC_{12}^j	1.64	Coffee	RC
VIII	66	SC_{12}	2.1	Wine	FC[k]

Adopting this picture, provisionally, leads to the following arithmetic relation for the number of free-valence-conduction electrons of an $[\mathrm{Au}_n(\mathrm{SR})_m]^{z-}$ cluster compound:

$$n_e = n_{\mathrm{Au}} - m_{SR} + z.$$

The counting given in Table 1 shows how known or reasonable values (for n, m and z) can give greatly reduced electron-counts, as well as agreement with shell-closings. The fraction (n_e/n_{Au}) falls strongly with decreasing cluster size, e.g. to 18/44 in the case of the recently isolated gold-cluster benzene-thiolate compound [18], much as the integrated intensity does. Naturally, such a drastically simplified and speculative model will be challenged by new evidence; but its utility here in reconciling the spectroscopic functions and integrals is evident enough.

The authors acknowledge contributions from Profs. Michel Broyer and Walter deHeer, who respectively provided access to unpublished calculations and critical discussion of the resonant absorption models.

References

1. For recent reviews, see: J.C. Love, L.A. Estroff, J.K. Kriebel, R.G. Nuzzo, G.M. Whitesides, Chem. Rev. **105**, 1103 (2005); M. Daniel, D. Astruc, Chem. Rev. **104**, 293 (2004); U. Kriebig, M. Vollmer, *Optical Properties of Metal Clusters* (Spinger, Berlin, 1995); A.C. Templeton, M.P. Wuelfing, R.W. Murray, Acc. Chem. Res. **33**, 27 (2000)
2. Portions of these results have been presented in earlier, fragmentary reports: S.-W. Chen et al., Science **280**, 2098 (1999); J.T. Khoury, Ph.D. thesis, University of California Los Angeles, 1999; R. Wyrwas, Ph.D. thesis, Georgia Institute of Technology, 2004

3. T.G. Schaaff, Anal. Chem. **76**, 6187 (2004); Y. Negishi, Y. Takasugi, S. Sato, H. Yao, K. Kimura, T. Tsukuda, J. Am. Chem. Soc. **126**, 6518 (2004)
4. M.M. Alvarez, J.T. Khoury, T.G. Schaaff, M.N. Shafigullin, I. Vezmar, R.L. Whetten, J. Phys. Chem. B **101**, 3706 (1997); R.L. Whetten, J.T. Khoury, M.M. Alvarez, S. Murthy, I. Vezmar, Z.L. Wang, P.W. Stephens, C.L. Cleveland, W.D. Luedtke, U. Landman, Adv. Mater. **8**, 428 (1996); T.G. Schaaff, M.N. Shafigullin, J.T. Khoury, I. Vezmar, R.L. Whetten, J. Phys. Chem. B **105**, 8785 (2001)
5. T.G. Schaaff, R.L. Whetten, J. Phys. Chem. B **104**, 2630 (2000), and references therein
6. C.F. Bohren, D.R. Huffman, *Absorption and Scattering of Light by Small Particles* (John Wiley and Sons, New York, 1983), p. 117
7. Y. Negishi, K. Nobusada, T. Tsukuda, J. Am. Chem. Soc. **127**, 5261 (2005)
8. M.Z. Quinten, Phys. B **101**, 211 (1996)
9. M. Valden, X. Lai, D.W. Goodman, Science **281**, 1647 (1998); Y. Maeda, M. Okumura, S. Tsubota, M. Kohyama, M. Haruta, Appl. Surf. Sci. **222**, 409 (2004); M. Chen, D.W. Goodman, Acc. Chem. Res. **39**, 739 (2006)
10. W. Ekardt, Phys. Rev. B **31**, 6360 (1985)
11. A. Rubio, L.C. Balbas, J.A. Alonso, Phys. Rev. B **46**, 4891 (1992)
12. L. Jdira, P. Liljeroth, E. Stoffels, D. Vanmaekelbergh, S. Speller, Phys. Rev. B **73**, 115305 (2006)
13. W.A. deHeer, Rev. Mod. Phys. **65**, 611 (1993)
14. E. Cottancin, G. Celep, J. Lermé, M. Pellarin, J.R. Huntzinger, J.L. Vialle, M. Broyer, Theor. Chem. Acc. **116**, 514 (2006) and references therein
15. I.L. Garzon et al., Phys. Rev. Lett. **85**, 5250 (2000)
16. H. Häkkinen, M. Walter, H. Grönbeck, J. Phys. Chem. B **110**, 9927 (2006); B. Yoon, P. Koskinen, B. Huber, O. Kostko, B. von Issendorff, H. Häkkinen, M. Moseler, U. Landman, Chem. Phys. Phys. Chem. **8**, 157 (2007)
17. H. Grönbeck, M. Walter, H. Häkkinen, J. Am. Chem. Soc. **128**, 10268 (2006)
18. R.C. Price, R.L. Whetten, J. Am. Chem. Soc. **127**, 13750 (2005); R.C. Price, R.L. Whetten, J. Phys. Chem. B **110**, 22166 (2006)